Max-Planck-Institut für Mathematik in den Naturwissenschaften Leipzig

Fast and Accurate 3D Tensor Calculation of the Fock Operator in a General Basis

(revised version: June 2012)

by

Venera Khoromskaia, Dirk Andrae, and Boris N. Khoromskij

Preprint no.: 4 2012

Fast and Accurate 3D Tensor Calculation of the Fock Operator in a General Basis

V. KHOROMSKAIA,* D. ANDRAE,** B.N. KHOROMSKIJ◇

Abstract

The present paper contributes to the construction of a "black-box" 3D solver for the Hartree-Fock equation by the grid-based tensor-structured methods. It focuses on the calculation of the Galerkin matrices for the Laplace and the nuclear potential operators by tensor operations using the generic set of basis functions with low separation rank, discretized on a fine $N \times N \times N$ Cartesian grid. We prove the Ch^2 error estimate in terms of mesh parameter, $h = O(1/N)$, that allows to gain a guaranteed accuracy of the core Hamiltonian part in the Fock operator as $h \to 0$. However, the commonly used problem adapted basis functions have low regularity yielding a considerable increase of the constant C, hence, demanding rather large grid-size N of about several tens of thousands to ensure the high resolution. Modern tensor-formatted arithmetics of complexity $O(N)$, or even $O(\log N)$, practically relaxes the limitations on the grid-size. Our tensor-based approach allows to improve significantly the standard basis sets in quantum chemistry by including simple combinations of Slater-type, local finite element and other basis functions. Numerical experiments for moderate size organic molecules show efficiency and accuracy of grid-based calculations to the core Hamiltonian in the range of grid parameter $N^3 \sim 10^{15}$.

AMS Subject Classification: 65F30, 65F50, 65N35, 65F10
Key words: tensor-structured methods, Hartree-Fock equation, grid-based tensor approximation, error estimates.

1 Introduction

This paper presents the method for grid-based calculations of the core Hamiltonian part of the Fock operator in the Hartree-Fock equation. It completes the concept of the numerical solution to the Hartree-Fock equation by the tensor-structured methods introduced in [1, 2, 3]. This approach does not assume the "sparsified" precomputation of the two-electron integrals, but instead, the Hartree and exchange operators are calculated "on the fly", in the

*Max-Planck-Institute for Mathematics in the Sciences, Inselstr. 22-26, D-04103 Leipzig, Germany (vekh@mis.mpg.de).

**Institute of Chemistry and Biochemistry, Freie Universität Berlin, Takustr. 3, D-14195 Berlin, Germany (dirk.andrae@fu-berlin.de).

◇Max-Planck-Institute for Mathematics in the Sciences, Inselstr. 22-26, D-04103 Leipzig, Germany (bokh@mis.mpg.de).

course of a self-consistent field iteration. Tensor methods eliminate the usual restrictions of analytical integrability for the approximating basis, hence providing the way to application of rather general physically relevant grid-based basis sets.

Another concepts to the grid-based approximation of the Hartree-Fock equation are based on multiresolution analysis [4, 5] that employes the separable representation to the Newton potential in the calculation of some integrals, wavelet approximation [31] or on domain decomposition techniques [12]. We also refer to [6] on a direct method for calculating the Hartree potential employing the Poisson equation, with $O(N^{4/3})$ complexity, where N is the univariate grid size.

Traditionally, the solution of the Hartree-Fock problem for a general molecule by grid-based approaches was considered untractable due to the large number of grid points in the 3D computational box required. Exceptions are the single atom [7, 8, 9], diatomic [10, 11] and linear molecules [12], where the dimensionality of the problem can be reduced to a one- or two-dimensional scheme, with the grid points being placed exactly at the positions of the atomic nuclei. Therefore, for general multinuclear systems, the naturally separable bases consisting of analytically integrable Gaussians are the cornerstone of most *ab initio* packages in molecular electronic structure calculations. At the same time, although building the accurate bases has been always a prerogative of experienced specialists, there are inavoidable difficulties on this way further, due to instability of the natural bases when increasing accuracy, and the steep increase in basis set size when larger molecules with heavier nuclei are to be treated.

At present, for the solution of the multidimensional problems on large $N \times ... \times N$ d-dimensional grids, the novel tensor-structured methods are developed [1, 2, 3, 13], having the complexity scaling $O(dN)$. Hence the number of grid points is not an issue anymore, and one can try to reconsider some of the numerical bottlenecks in the traditional tasks of quantum chemistry from a different point of view. Note that using the quantized tensor representations [14], one can expect nearly mesh-independent grid-based calculations of log-volume complexity $O(d \log N)$ in the problems of quantum chemistry.

In this paper, the computation of the Galerkin matrices for the Laplace and the nuclear potential operators is introduced, using a discretized representation of the molecular basis functions on fine $N \times N \times N$ Cartesian grids.

The Galerkin integrals for the Laplace operator are calculated numerically by the tensor-structured operations of $1D$ compexity, $O(N) \ll N^3$, that allow extremely large grid-sizes required for high resolution of Gaussian "needles" in evaluation of the 3D finite-difference Laplacian. As a result, we obtain a fully populated Laplace matrix of size $N_b \times N_b$ for the given set of N_b basis functions (2.6) represented by piecewise linear finite elements on fine 3D Cartesian grids. The numerical tensor concept essentially relaxes the constraints on the selection of basis sets, allowing rather general physically relevant functions with low separation rank, represented by their values on the grid. This becomes possible since the functional calculus, including numerical differentiation and integration, is performed via the rank-structured multilinear algebra (see §4 and Appendix 1). Thus, basis sets can be improved significantly, for example, by enhancement via a few local finite elements situated in the nuclei cusps, or by including Slater-type functions representing the dominating singularities, etc. In particular, we give an example of constructing a basis in a "black-box" way using the expansion of a Slater function by the parametric sinc-approximation, where the

accuracy of approximation can be easily controlled by the choice of rank parameters and the grid size N.

The tensor-structured calculation of the nuclear potential operator is reduced to $1D$ Hadamard and scalar products of the grid-based basis functions and the low-rank representation of the nuclear potential. The latter is designed by using the sinc-quadrature approximation to the Newton potential as in [15]. Applying this construction multiple times, but shifted with respect to the coordinates of nuclei, we get the resulting operator as the Galerkin projection of a sum of the canonical tensors approximating the individual Newton kernels. In the case of large molecules, the ultimate tensor rank of the nuclear potential sum can be adaptively truncated by the reduced higher order singular value decomposition (RHOSVD) introduced in [1].

We prove the $O(h^2)$-error effected by the piecewise linear grid interpolation with mesh parameter $h = O(1/N)$. Hence, choosing N large enough, one gains a guaranteed accuracy of tensor computations for the core Hamiltonian part in the Fock operator. The numerical complexity scales quadratically in the separation ranks of basis functions, R_b, and linearly (log-linearly) in the grid-size N.

Our approach for fast and accurate calculation[1] of the kinetic and the nuclear potential operators is approved by the numerical tests over fine 3D Cartesian grids, with the univariate grid-size N in the range $N \leq 2^{19}$. This corresponds to the box volume with the number of entries N^3 of order $2^{57} \sim 10^{17}$, and with a step-size of about 10^{-5} Å $= 10^{-15}$ m $= 1$ fm, ensuring high resolution. Note that this femtometer range of the mesh size h is compatible with the size of the atomic nucleus.

The rest of the article is organized as follows. In §2 we recall the Galerkin scheme for the numerical approximation to the Hartree-Fock equation, with an emphasis on the tensor calculus interpretation. §3 outlines the tensor-structured schemes for calculation of the Coulomb and exchange matrices in the Fock operator reported in [2, 3]. §4 presents the main result of this paper, the tensor numerical scheme for the core Hamiltonian part, including the Laplace operator and the nuclear potential. §6 shows numerics on the fully discrete grid-based calculation of the core Hamiltonian, first, on the example of the Schrödinger equation for the hydrogen atom, using both the standard Gaussian basis with fixed accuracy, and an automatically generated sinc-quadrature basis providing the controllable precision. We illustrate the effect of the augmented basis by including the local piecewise linear hat functions. Further, in §6 we present the numerical results for the Laplace and nuclear potential Galerkin matrices for compact (3D) organic molecules of moderate size, and compare them with the outputs of standard quantum chemical calculations (obtained with the MOLPRO package [16]). For completeness, in §6.4 we sketch the algorithm of the tensor-structured numerical solution to the Hartree-Fock equation [3], and the corresponding flow-chart. §6 resumes the main results. In Appendix 1 we provide the error analysis of our discretization scheme in the case of piecewise constant/linear approximations.

[1] Computations are implemented in MATLAB.

2 The Galerkin scheme for the Hartree-Fock equation

The Hartree-Fock equations are orbital equations obtained within a mean-field approximation to the many-electron problem [17]. They are derived from application of the variational principle to the expectation value of the many-electron Hamiltonian over a configuration state function (CSF) characterizing the desired state of the many-electron system under study. In simple cases, like the ground state of a closed-shell system (n_{elec} electrons, n_{elec} even) to which we restrict ourselves here, this CSF reduces to a single Slater determinant built up from the orbitals. The Hartree-Fock equations then read (for orthonormal orbitals)

$$\mathcal{F}\psi_i(x) = \lambda_i\,\psi_i(x), \quad \int_{\mathbb{R}^3} \psi_i\psi_j dx = \delta_{ij}, \quad i,j = 1,...,N_{orb}{=}\, n_{elec}/2, \tag{2.1}$$

which constitutes an eigenvalue problem for the (atomic or molecular) orbitals ψ_i. Here $\mathcal{F}$ is the nonlinear Fock operator on $H^1(\mathbb{R}^3)$,

$$\mathcal{F} := -\frac{1}{2}\Delta + V_c + V_H - \mathcal{K}, \tag{2.2}$$

with the nuclear potential

$$V_c(x) = -\sum_{\nu=1}^{M} \frac{Z_\nu}{\|x - a_\nu\|}, \quad Z_\nu > 0, \;\; a_\nu \in \mathbb{R}^3, \tag{2.3}$$

and where both the Hartree potential $V_H(x)$ and the nonlocal exchange operator $\mathcal{K}$ are functions of the desired solution of (2.1),

$$V_H(x) := \int_{\mathbb{R}^3} \frac{\rho(y)}{\|x-y\|}\, dy, \quad x \in \mathbb{R}^3, \tag{2.4}$$

and

$$(\mathcal{K}\psi)(x) := \frac{1}{2}\int_{\mathbb{R}^3} \frac{\tau(x,y)}{\|x-y\|}\,\psi(y)dy, \tag{2.5}$$

such that the density matrix $\tau(x,y)$, and electron density $\rho(x)$, are given by

$$\tau(x,y) := 2\sum_{a=1}^{N_{orb}} \psi_a(x)\psi_a(y), \quad \rho(x) := \tau(x,x).$$

The standard Galerkin scheme applied to the initial problem in form (2.1) is posed in $H^1(\mathbb{R}^3)$ [18]. Using expansion of the molecular orbitals in the given basis set $\{g_m\}_{1\le m\le N_b}$,

$$\psi_a(x) = \sum_{m=1}^{N_b} c_{ma} g_m(x), \quad a = 1,...,N_{orb}, \tag{2.6}$$

we obtain the following representations, which happen to be useful for further tensor-structured calculations of the density matrix,

$$\tau(x,y) = 2\sum_{a=1}^{N_{orb}} \psi_a(x)\psi_a(y) = 2\sum_{a=1}^{N_{orb}} \left(\sum_{m=1}^{N_b} c_{ma} g_m(x)\right)\left(\sum_{m=1}^{N_b} c_{ma} g_m(y)\right),$$

and the respective representation of $\rho(x)$. Consequently, we have

$$V_H(x) = \rho * \frac{1}{\|\cdot\|}(x) = \int_{\mathbb{R}^3} \sum_{a=1}^{N_{orb}} \frac{\left(\sum_{m=1}^{N_b} c_{ma} g_m(y)\right)^2}{\|x-y\|} dy.$$

The stiffness matrix $H = \{h_{\mu\nu}\}$ of the core Hamiltonian part $\mathcal{H} = -\frac{1}{2}\Delta + V_c$,

$$h_{\mu\nu} = \frac{1}{2}\int_{\mathbb{R}^3} \nabla g_\mu \cdot \nabla g_\nu dx + \int_{\mathbb{R}^3} V_c(x) g_\mu g_\nu dx, \quad 1 \le \mu, \nu \le N_b,$$

includes the kinetic energy of electrons and the nuclear-electron interaction potential.

Then, the Galerkin representation leads to the Hartree, $J(C)$, and exchange, $K(C)$, matrices expressed entrywise in terms of the coefficients matrix $C = \{c_{ma}\}$ as

$$J(C)_{\mu\nu} = \int_{\mathbb{R}^3} V_H(x) g_\mu(x) g_\nu(x) dx = \langle V_H, g_\mu g_\nu \rangle_{L^2(\mathbb{R}^3)} \tag{2.7}$$

and

$$\begin{aligned} K(C)_{\mu\nu} &= -\frac{1}{2}\iint_{\mathbb{R}^3} \frac{\tau(x,y)}{\|x-y\|} g_\nu(y) g_\mu(x) dy dx \qquad (2.8)\\ &= -\sum_{a=1}^{N_{orb}} \iint_{\mathbb{R}^3} \frac{g_\nu(y)\left(\sum_{m=1}^{N_b} c_{ma} g_m(y)\right)}{\|x-y\|} g_\mu(x) \left(\sum_{m=1}^{N_b} c_{ma} g_m(x)\right) dy dx, \end{aligned}$$

respectively. The complete Fock matrix $F = F(C)$ is then given by

$$F(C) = H + G(C), \quad G(C) = J(C) + K(C), \tag{2.9}$$

yielding the Galerkin equation for the Hartree-Fock eigenvalue problem,

$$\begin{aligned} FC = SC\Lambda, \quad \Lambda = \mathrm{diag}(\lambda_1, ..., \lambda_{N_b}), \qquad (2.10)\\ C^* SC = I_{N_b}, \quad I_{N_b} \in \mathbb{R}^{N_b \times N_b} \end{aligned}$$

where the second equation represents the orthogonality constraints $\int_{\mathbb{R}^3} \psi_i \psi_j = \delta_{ij}$ and

$$S = \{\int_{\mathbb{R}^3} g_\nu(x) g_\mu(x) dx\}$$

is the Galerkin mass matrix.

3 Rank-structured tensor formats

The core of our method is the low-rank tensor representation of arising functions and operators on $N \times N \times N$ Cartesian grid, and implementation of the corresponding multi-linear algebraic operations in the tensor product format.

A tensor of order d is a multidimensional array of real (complex) data whose elements are referred by using a tensor-product index set $\mathcal{I} = I_1 \times \ldots \times I_d$,

$$\mathbf{A} = [a_{i_1,\ldots,i_d} : i_\ell \in I_\ell] \in \mathbb{R}^{\mathcal{I}}, \quad I_\ell = \{1, ..., N_\ell\}, \quad \ell = 1, ..., d.$$

Assume for simplicity that $N_\ell = N$ for all $\ell = 1, ..., d$, then the number of entries in $\mathbf{A}$ amounts to N^d, hence increasing exponentially in d. To get rid of exponential scaling in the dimension, one can apply the approximate rank structured representations of multidimensional tensors. As the simplest rank structured ansatz, the *tensor product* of vectors $u_\ell = \{u_{\ell,i_\ell}\}_{i_\ell \in I_\ell} \in \mathbb{R}^{I_\ell}$ $(\ell = 1, ..., d)$ is used, that forms the canonical rank-1 tensor,

$$\mathbf{A} \equiv [u_{\mathbf{i}}]_{\mathbf{i}\in\mathcal{I}} = u_1 \otimes ... \otimes u_d \in \mathbb{R}^{\mathcal{I}} \quad \text{with entries} \quad u_{\mathbf{i}} = u_{1,i_1} \cdots u_{d,i_d},$$

which requires only dN numbers to store it. A tensor in the canonical format is defined as

$$\mathbf{A}_{(R)} = \sum_{k=1}^{R} c_k u_k^{(1)} \otimes \ldots \otimes u_k^{(d)}, \quad c_k \in \mathbb{R}, \tag{3.1}$$

where $u_k^{(\ell)}$ are normalised vectors, and R is called the canonical rank of a tensor. Given the rank parameter $\mathbf{r} = (r_1, ..., r_d)$, the initial tensor $\mathbf{A}$ can be represented in the so-called Tucker format

$$\mathbf{A} \approx \mathbf{A}_{(\mathbf{r})} = \sum\nolimits_{\nu_1=1}^{r_1} \ldots \sum\nolimits_{\nu_d=1}^{r_d} \beta_{\nu_1,\ldots,\nu_d}\, v_{\nu_1}^{(1)} \otimes \ldots \otimes v_{\nu_d}^{(d)},$$

with the orthonormal vectors $v_{\nu_\ell}^{(\ell)} \in \mathbb{R}^{I_\ell}$ $(1 \le \nu_\ell \le r_\ell)$. The parameter $r = \max\limits_{\ell}\{r_\ell\}$ is called the Tucker rank, and the coefficients tensor $\boldsymbol{\beta} = [\beta_{\nu_1,\ldots,\nu_d}]$ is called the core tensor (usually for function related tensors, $r \ll N$).

Rank-structured tensor representation allows efficient reduction of storage and fast multilinear algebra, see [26] and references therein. Here we briefly recall the multilinear algebra operations for tensors $\mathbf{A}_1$, $\mathbf{A}_2$, represented in the rank-R canonical format, (3.1),

$$\mathbf{A}_1 = \sum_{k=1}^{R_1} c_k u_k^{(1)} \otimes \ldots \otimes u_k^{(d)}, \quad \mathbf{A}_2 = \sum_{m=1}^{R_2} b_m v_m^{(1)} \otimes \ldots \otimes v_m^{(d)}, \tag{3.2}$$

with normalized vectors $u_k^{(\ell)}, v_m^{(\ell)} \in \mathbb{R}^{I_\ell}$. (For simplicity of notation, we consider $N_\ell = N$.) For given canonical tensors $\mathbf{A}_1$, $\mathbf{A}_2$, the Eucledian scalar product can be computed by

$$\langle \mathbf{A}_1, \mathbf{A}_2 \rangle := \sum_{k=1}^{R_1} \sum_{m=1}^{R_2} c_k b_m \prod_{\ell=1}^{d} \left\langle u_k^{(\ell)}, v_m^{(\ell)} \right\rangle,$$

leading to complexity $O(dNR_1R_2)$. The Hadamard product of two multidimensional tensors $\mathbf{A}_1, \mathbf{A}_2$ given in the canonical format (3.2) is calculated by

$$\mathbf{A}_1 \odot \mathbf{A}_2 := \sum_{k=1}^{R_1} \sum_{m=1}^{R_2} c_k b_m \left(u_k^{(1)} \odot v_m^{(1)}\right) \otimes \ldots \otimes \left(u_k^{(d)} \odot v_m^{(d)}\right),$$

with complexity $O(dNR_1R_2)$.

In electronic structure calculations, the three-dimensional convolution transform with the Newton convolving kernel, $\frac{1}{\|x-y\|}$, is the most computationally expensive operation. We employ the tensor-structured computation of this transform over large $N \times N \times N$ Cartesian grid with $O(N \log N)$ complexity introduced in [19]. Approximating the function related tensor $\mathbf{A}_1 = \mathbf{F}$ in the rank-R_1 canonical format (3.1), and the Newton potential $\mathbf{A}_2 = \mathbf{P}$ by the canonical rank-R_2 tensor enables us to compute $\mathbf{F} * \mathbf{F}$ in the form

$$\mathbf{F} * \mathbf{P} = \sum_{k=1}^{R_1} \sum_{m=1}^{R_2} c_k b_m \left(u_k^{(1)} * v_m^{(1)} \right) \otimes \left(u_k^{(2)} * v_m^{(2)} \right) \otimes \left(u_k^{(3)} * v_m^{(3)} \right),$$

leading to complexity of the 3D convolution, $O(R_1 R_2 N \log N)$. The tensor product convolution considerably outperforms the conventional 3D FFT-base algorithm having the complexity $O(N^3 \log N)$, see numerics in [3].

When using the rank-structured representations of functions and operators in the Hartree-Fock equation, the 3D and 6D integrations are replaced by multilinear algebra operations such as the scalar and Hadamard products, the 3D convolution transforms which are implemented with an almost $O(N)$-complexity [1, 20]. However, the rank-structured operations mandatory lead to increase of tensor ranks. For tensor rank reduction we use the robust algorithm based on the canonical-to-Tucker and Tucker-to-canonical transforms for 3D tensors introduced in [1], which is also of linear complexity with respect to parameters of the target canonical tensor, $O(RN)$.

The combination of the canonical and Tucker tensor formats is useful in 3D applications. The rank-structured tensor formats suitable for problems in higher dimensions include the matrix-product states (MPS) [32, 33], TT format [34, 35] and the quantized-TT (QTT) approximation which is of $O(\log N)$ complexity (see also [36]).

4 Tensor computation of the Coulomb and exchange matrices

In this section we recall the tensor numerical scheme for calculation of the Coulomb and exchange matrices, discussed in full detail in the previous papers [1, 2, 3].

Suppose that the initial eigenvalue problem (2.1) is posed in the finite volume box

$$\Omega = [-b, b]^3 \in \mathbb{R}^3, \tag{4.1}$$

subject to the homogeneous Dirichlet boundary conditions on $\partial\Omega$. This assumption is justified by the exponential decay of the orbitals $\psi_i(x)$ as $\|x\| \to \infty$.

For given discretization parameter $n \in \mathbb{N}$, introduce the equidistant tensor grid $\omega_{\mathbf{3},n}$ with the mesh-size $h = 2b/n$, and define the set of piecewise constant basis functions (indicator functions) $\{\zeta_{\mathbf{i}}\}$, $\mathbf{i} \in \mathcal{I} := \{1, ..., n\}^3$, associated with the respective grid-cells in $\omega_{\mathbf{3},n}$. This allows to introduce the set of cell-centered collocation discretizations, $\{\overline{g}_k\}$, to the continuous basis functions $g_k(x)$ by piecewise constant interpolation,

$$\mathbf{I}_0 : g_k \to \overline{g}_k := \sum_{\mathbf{i} \in \mathcal{I}} g_k(x_{\mathbf{i}}) \zeta_{\mathbf{i}}(x),$$

where $g_k(x_{\mathbf{i}})$ is the cell-centered sampling of g_k. Assuming for the ease of presentation that g_k is rank-1 separable, i.e., $g_k(x) = \prod_{\ell=1}^{3} g_k^{(\ell)}(x_\ell)$, one obtains the separable piecewise constant representation to the initial basis functions,

$$g_k(x) \approx \mathbf{I}_0 g_k := \overline{g}_k(x) = \prod_{\ell=1}^{3} \overline{g}_k^{(\ell)}(x_\ell) = \prod_{\ell=1}^{3} \sum_{i=1}^{n} g_k^{(\ell)}(x_{i_\ell}) \zeta_i^{(\ell)}(x_\ell), \tag{4.2}$$

with the rank-1 coefficients tensor given by $\mathbf{G}_k = G_k^{(1)} \otimes G_k^{(2)} \otimes G_k^{(3)}$, having the canonical vectors $G_k^{(\ell)} = g_k^{(\ell)}(x_{i_\ell})$, obtained by the univariate cell-centered collocation.

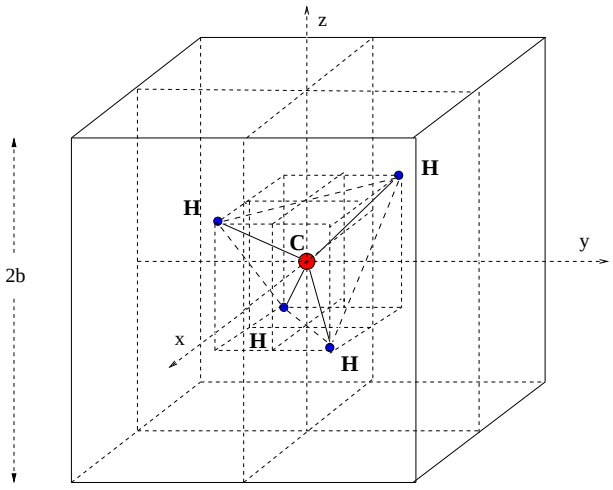

Figure 4.1: Computational box for the CH_4 molecule.

The tensor-structured computational scheme for the Coulomb matrix (2.7) can be written by the following tensor operations [2, 3]. The electron density is represented by a low-rank canonical tensor,

$$\rho \approx \boldsymbol{\rho} := \sum_{a=1}^{N_{orb}} \left(\sum_{\kappa,\lambda=1}^{N_b} c_{\kappa a} c_{\lambda a} \mathbf{G}_\kappa \odot \mathbf{G}_\lambda \right),$$

and the Hartree potential by the tensor-product convolution [19]

$$V_H = \rho * \frac{1}{\| \cdot \|} \approx \boldsymbol{\rho} * \mathbf{P}_N, \quad \mathbf{P}_N \approx \{ \langle \frac{1}{\| \cdot \|} \zeta_{\mathbf{i}}, \zeta_{\mathbf{j}} \rangle \}, \quad \mathbf{i}, \mathbf{j} \in \mathcal{I}, \tag{4.3}$$

where $\mathbf{P}_N \in \mathbb{R}^{\mathcal{I}}$ is the low-rank representation (approximation) to the projection coefficient tensor for the Newton potential (we denote $rank(\mathbf{P}_N) = R_N$). The tensor calculation of the Coulomb matrix in (2.7) is obtained by

$$J(C)_{\mu\nu} = \langle \overline{g}_\mu(x) \overline{g}_\nu(x), V_H(x) \rangle \approx \langle \mathbf{G}_\mu \odot \mathbf{G}_\nu, \boldsymbol{\rho} * \mathbf{P}_N \rangle, \quad 1 \le \mu, \nu \le N_b. \tag{4.4}$$

In the case of a Gaussian basis set, the canonical $rank(\mathbf{G}_\mu) = 1$, while, in general, we have $R_\mu = rank(\mathbf{G}_\mu) \ge 1$. In turn, 3rd order tensors $\boldsymbol{\rho}$ and $\mathbf{P}_N$ are to be approximated by low-rank tensors.

First, we represent the matrix $K(C)$ using tensor operations by the following three loops, as shown in [20, 3]. For $a = 1, ..., N_{orb}$, and $\nu = 1, ..., N_b$, compute the convolution integrals,

$$W_{a\nu}(x) = \int\limits_{\mathbb{R}^3} \frac{\overline{g}_\nu(y) \sum\limits_{m=1}^{N_b} c_{ma}\overline{g}_m(y)}{\|x-y\|} dy \tag{4.5}$$

$$\approx \boldsymbol{W}_{a\nu} := \left[\mathbf{G}_\nu \odot \sum_{m=1}^{N_b} c_{ma}\mathbf{G}_m\right] * \mathbf{P}_N,$$

and then the scalar products ($\mu, \nu = 1, ..., N_b$),

$$K_{\mu\nu,a} = \int_{\mathbb{R}^3} \left[\sum_{m=1}^{N_b} c_{ma}\overline{g}_m(x)\right] \overline{g}_\mu(x) W_{a\nu}(x) dx \tag{4.6}$$

$$\approx \boldsymbol{K}_{\mu\nu,a} := \langle \mathbf{G}_\mu \odot \left[\sum_{m=1}^{N_b} c_{ma}\mathbf{G}_m\right], \boldsymbol{W}_{a\nu}\rangle.$$

Finally, the entries of the exchange matrix are given by sums over all orbitals,

$$K(C)_{\mu\nu} = \sum_{a=1}^{N_{orb}} K_{\mu\nu,a}, \quad \mu, \nu = 1, ..., N_b. \tag{4.7}$$

This scheme gains from efficient low-rank separable approximation of the Newton kernel, the discretized electron density $\rho(x)$, and of auxiliary potentials $W_{a\nu}(x)$ at step (4.5), that ensures low complexity of the three-dimensional tensor-structured operations including rank reduction algorithms.

5 Tensor calculus for core Hamiltonian

Here we present the grid-based calculation of the core Hamiltonian part in the Fock operator (2.2),

$$\mathcal{H} = -\frac{1}{2}\Delta_{(3)} + V_c,$$

with respect to the Galerkin basis $\{g_m(x)\}_{1\le m\le N_b}, x \in \mathbb{R}^3$, where $V_c(x)$ is given by (2.3) and $\Delta_{(3)}$ represents the 3D Laplacian.

5.1 Laplace operator

The initial eigenvalue problem is posed in the finite volume box $\Omega = [-b, b]^3 \in \mathbb{R}^3$, as in (4.1), subject to the homogeneous Dirichlet boundary conditions on $\partial\Omega$. For given discretization parameter $N \in \mathbb{N}$, we use the equidistant $N \times N \times N$ tensor grid $\omega_{\mathbf{3},N} = \{x_\mathbf{i}\}$, $\mathbf{i} \in \mathcal{I} := \{1, ..., N\}^3$, with the mesh-size $h = 2b/(N+1)$, which might be different from the grid $\omega_{\mathbf{3},n}$ introduced in §3 (usually, $n \le N$).

Now, similar to Section 3, define a set of piecewise linear basis functions $\overline{g}_k := \mathbf{I}_1 g_k$, $k = 1, ..., N_b$, by linear tensor-product interpolation via the set of product hat functions, $\{\xi_{\mathbf{i}}\} = \xi_{i_1}(x_1)\xi_{i_2}(x_2)\xi_{i_3}(x_3)$, $\mathbf{i} \in \mathcal{I}$, associated with the respective grid-cells in $\omega_{\mathbf{3},N}$. Here the linear interpolant $\mathbf{I}_1 = I_1 \times I_1 \times I_1$ is a product of 1D interpolation operators, $\overline{g}_k^{(\ell)} = I_1 g_k^{(\ell)}$, $\ell = 1, ..., 3$, where $I_1 : C^0([-b, b]) \to W_h := span\{\xi_i\}_{i=1}^N$ is defined over the set of piecewise linear basis functions by

$$(I_1\, w)(x_\ell) := \sum_{i=1}^{N} w(x_{i_\ell})\xi_i(x_\ell), \quad x_{\mathbf{i}} \in \omega_{\mathbf{3},N}.$$

This leads to the separable grid-based approximation of the initial basis functions $g_k(x)$,

$$g_k(x) \approx \overline{g}_k(x) = \prod_{\ell=1}^{3} \overline{g}_k^{(\ell)}(x_\ell) = \prod_{\ell=1}^{3} \sum_{i=1}^{N} g_k^{(\ell)}(x_{i_\ell})\xi_i(x_\ell), \tag{5.1}$$

where the rank-1 coefficients tensor $\mathbf{G}_k$ is given by $\mathbf{G}_k = G_k^{(1)} \otimes G_k^{(2)} \otimes G_k^{(3)}$, with the canonical vectors $G_k^{(\ell)} = \{g_{k_i}^{(\ell)}\} \equiv \{g_k^{(\ell)}(x_{i_\ell})\}$ (see Figure 5.1 illustrating the construction of $\overline{g}_k(x_1)$).

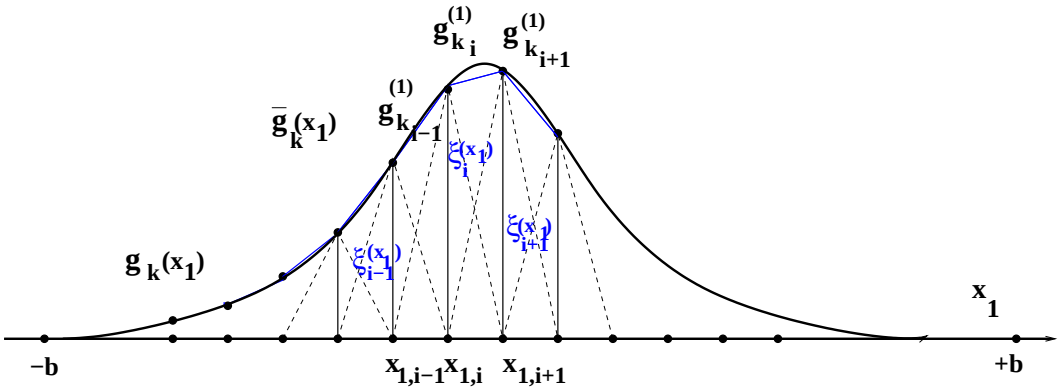

Figure 5.1: Using hat functions $\xi_i(x_1)$ for a single-mode basis function $g_k(x_1)$, yielding the piecewise linear representation $\overline{g}_k(x_1)$ of a continuous function $g_k(x_1)$.

We approximate the exact Galerkin matrix $A_g \in \mathbb{R}^{N_b \times N_b}$,

$$A_g = \{a_{km}\} := \{\langle -\Delta_{(3)} g_k, g_m \rangle\} \equiv \{\langle \nabla_{(3)} g_k, \nabla_{(3)} g_m \rangle\}, \quad k, m = 1, \dots N_b,$$

using the piecewise linear representation of the basis functions, $\overline{g}_k(x) \in \mathbb{R}^3$, see (5.1), constructed on $N \times N \times N$ Cartesian grid (see [30] for general theory of finite element approximation). Here $\nabla_{(3)}$ denotes the 3D gradient operator. The approximating matrix A_G is now defined by

$$A_g \approx A_G = \{\overline{a}_{km}\} := \{\langle -\Delta_{(3)} \overline{g}_k, \overline{g}_m \rangle\} \equiv \{\langle \nabla_{(3)} \overline{g}_k, \nabla_{(3)} \overline{g}_m \rangle\}, \quad A_G \in \mathbb{R}^{N_b \times N_b}. \tag{5.2}$$

The accuracy of this approximation is of order $\|a_{km} - \overline{a}_{km}\| = O(h^2)$, where h is the mesh size, see Theorem 8.4 and numerics in §6.

Recall that the Laplace operator applies to a separable function $\eta(x), x = (x_1, x_2, x_3) \in \mathbb{R}^3$, having a represention $\eta(x) = \eta_1(x_1)\eta_2(x_2)\eta_3(x_3)$, as follows

$$\Delta_{(3)}\eta(x) = \frac{d^2\eta_1(x_1)}{dx_1^2}\eta_2(x_2)\eta_3(x_3) + \frac{d^2\eta_2(x_2)}{dx_2^2}\eta_1(x_1)\eta_3(x_3) + \frac{d^2\eta_3(x_3)}{dx_3^2}\eta_1(x_1)\eta_2(x_2), \quad (5.3)$$

which ensures the rank-3 tensor representation of the respective Galerkin stiffness matrix A_3 in the tensor basis $\{\xi_i(x_1)\xi_j(x_2)\xi_k(x_3)\}$, $i, j, k = 1, \dots N$,

$$A_3 := A^{(1)} \otimes S^{(2)} \otimes S^{(3)} + S^{(1)} \otimes A^{(2)} \otimes S^{(3)} + S^{(1)} \otimes S^{(2)} \otimes A^{(3)} \in \mathbb{R}^{N^{\otimes 3} \times N^{\otimes 3}}.$$

Here the 1D stiffnesss and mass matrices $A^{(\ell)}, S^{(\ell)} \in \mathbb{R}^{N\times N}$, $\ell = 1, 2, 3$, are given by

$$A^{(\ell)} := \{\langle \nabla_{(1)}\xi_i(x_\ell), \nabla_{(1)}\xi_j(x_\ell)\rangle\}_{i,j=1}^N = \frac{1}{h} tridiag\{-1, 2, -1\},$$

$$S^{(\ell)} = \{\langle \xi_i, \xi_j\rangle\}_{i,j=1}^N = \frac{h}{6}\, tridiag\{1, 4, 1\},$$

respectively, and $\nabla_{(1)} = \frac{d}{dx_\ell}$. Since $\{\xi_i\}_{i=1}^N$ are the same for all modes $\ell = 1, 2, 3$, for simplicity of notation, we further assume, $A^{(\ell)} = A_1$, and $S^{(\ell)} = S_1$.

Lemma 5.1 *(Galerkin matrix A_G). Assume that the basis functions $\{\overline{g}_k(x)\}$, $x \in \mathbb{R}^3$, $k = 1, \dots N_b$, are rank-1 separable, i.e., $\overline{g}_k(x) = \overline{g}_k^{(1)}(x_1)\overline{g}_k^{(2)}(x_2)\overline{g}_k^{(3)}(x_3)$. Then the matrix entries of A_G have the representation,*

$$\begin{aligned} \overline{a}_{km} &= \langle A_1 G_k^{(1)}, G_m^{(1)}\rangle\langle S_1 G_k^{(2)}, G_m^{(2)}\rangle\langle S_1 G_k^{(3)}, G_m^{(3)}\rangle \\ &\quad + \langle S_1 G_k^{(1)}, G_m^{(1)}\rangle\langle A_1 G_k^{(2)}, G_m^{(2)}\rangle\langle S_1 G_k^{(3)}, G_m^{(3)}\rangle \\ &\quad + \langle S_1 G_k^{(1)}, G_m^{(1)}\rangle\langle S_1 G_k^{(2)}, G_m^{(2)}\rangle\langle A_1 G_k^{(3)}, G_m^{(3)}\rangle \\ &= \langle A_3 \mathbf{G}_k, \mathbf{G}_m\rangle, \end{aligned} \quad (5.4)$$

where $G_k^{(\ell)}$, $G_m^{(\ell)} \in \mathbb{R}^N$ $(k, m = 1, \dots, N_b)$, are the vectors of collocation coefficients of $\{\overline{g}_k^{(\ell)}(x_\ell)\}, \ell = 1, 2, 3$, and $\mathbf{G}_k$ are the corresponding rank-1 3-tensors $\mathbf{G}_k = G_k^{(1)} \otimes G_k^{(2)} \otimes G_k^{(3)}$, cf. (5.1).

Proof. By definition, we have

$$\overline{a}_{km} = \langle \nabla_{(3)}\overline{g}_k, \nabla_{(3)}\overline{g}_m\rangle = \langle \nabla_{(3)}(\overline{g}_k^{(1)}\overline{g}_k^{(2)}\overline{g}_k^{(3)}), \nabla_{(3)}\overline{g}_m^{(1)}\overline{g}_m^{(2)}\overline{g}_m^{(3)}\rangle.$$

Taking into account the representation (5.3), this implies,

$$\begin{aligned} \overline{a}_{km} &= \langle \nabla_{(1)}\overline{g}_k^{(1)}, \nabla_{(1)}\overline{g}_m^{(1)}\rangle\langle \overline{g}_k^{(2)}, \overline{g}_m^{(2)}\rangle\langle \overline{g}_k^{(3)}, \overline{g}_m^{(3)}\rangle \\ &+ \langle \overline{g}_k^{(1)}, \overline{g}_m^{(1)}\rangle\langle \nabla_{(1)}\overline{g}_k^{(2)}, \nabla_{(1)}\overline{g}_m^{(2)}\rangle\langle \overline{g}_k^{(3)}, \overline{g}_m^{(3)}\rangle \\ &+ \langle \overline{g}_k^{(1)}, \overline{g}_m^{(1)}\rangle\langle \overline{g}_k^{(2)}, \overline{g}_m^{(2)}\rangle\langle \nabla_{(1)}\overline{g}_k^{(3)}, \nabla_{(1)}\overline{g}_m^{(3)}\rangle. \end{aligned} \quad (5.5)$$

Simple calculations show that for $\ell = 1$,

$$\begin{aligned}\langle -\Delta_{(1)}\overline{g}_k^{(1)}, \overline{g}_m^{(1)}\rangle &= \langle \nabla_{(1)} \sum_{i=1}^{N} g_{ki}\xi_i(x_1), \nabla_{(1)} \sum_{j=1}^{N} g_{kj}\xi_j(x_1)\rangle \\ &= \langle \sum_{i=1}^{n} g_{ki}\nabla_{(1)}\xi_i(x_1), \sum_{j=1}^{N} g_{kj}\nabla_{(1)}\xi_j(x_1)\rangle \\ &= \sum_{i=1}^{N} g_{ki} \sum_{j=1}^{N} g_{kj}\langle \nabla_{(1)}\xi_i(x_1), \nabla_{(1)}\xi_j(x_1)\rangle = \langle A_1 G_k^{(1)}, G_m^{(1)}\rangle,\end{aligned}$$

and

$$\langle \overline{g}_k^{(1)}, \overline{g}_m^{(1)}\rangle = \langle S_1 G_k^{(1)}, G_m^{(1)}\rangle,$$

and similar for the remaining modes $\ell = 2, 3$. These representations imply

$$\overline{a}_{km} = \langle A_3 \mathbf{G}_k, \mathbf{G}_m\rangle,$$

which completes the proof. ■

Remark 5.2 *Agglomerating rank-*1 *vectors* $\mathbf{G}_k \in \mathbb{R}^{N^{\otimes 3}}$, $(k = 1, ..., N_b)$ *in a matrix* $G \in \mathbb{R}^{N^{\otimes 3} \times N_b}$, *the entrywise representation (5.4) can be written in a matrix form*

$$A_G = G^T A_3 G \in \mathbb{R}^{N_b \times N_b},$$

corresponding to the standard matrix-matrix transform under the change of basis.

Lemma 5.1 now implies that in case of basis functions having ranks larger than one,

$$g_m(x) = \sum_{p=1}^{R_m} \eta_p(x), \quad R_m \geq 1, \tag{5.6}$$

where $\eta_p(x)$ is the rank-1 separable function. Hence (5.4) takes form

$$\begin{aligned}\overline{a}_{km} = \sum_{p=1}^{R_k}\sum_{q=1}^{R_m} [&\langle A_1 G_{k,p}^{(1)}, G_{m,q}^{(1)}\rangle \langle S_1 G_{k,p}^{(2)}, G_{m,q}^{(2)}\rangle \langle S_1 G_{k,p}^{(3)}, G_{m,q}^{(3)}\rangle \\ &+ \langle S_1 G_{k,p}^{(1)}, G_{m,q}^{(1)}\rangle \langle A_1 G_{k,p}^{(2)}, G_{m,q}^{(2)}\rangle \langle S_1 G_{k,p}^{(3)}, G_{m,q}^{(3)}\rangle \\ &+ \langle S_1 G_{k,p}^{(1)}, G_{m,q}^{(1)}\rangle \langle S_1 G_{k,p}^{(2)}, G_{m,q}^{(2)}\rangle \langle A_1 G_{k,p}^{(3)}, G_{m,q}^{(3)}\rangle],\end{aligned} \tag{5.7}$$

where R_m, $m = 1, ..., N_b$, denote the rank parameters of the Galekin basis functions $\overline{g}_m$.

Representation (5.4) can be simplified by the standard lumping procedure preserving the same approximation error $O(h^2)$,

$$\begin{aligned}\overline{a}_{km} &= \langle A_1 G_k^{(1)}, G_m^{(1)}\rangle \langle G_k^{(2)}, G_m^{(2)}\rangle \langle G_k^{(3)}, G_m^{(3)}\rangle \\ &\quad + \langle G_k^{(1)}, G_m^{(1)}\rangle \langle A_1 G_k^{(2)}, G_m^{(2)}\rangle \langle G_k^{(3)}, G_m^{(3)}\rangle \\ &\quad + \langle G_k^{(1)}, G_m^{(1)}\rangle \langle G_k^{(2)}, G_m^{(2)}\rangle \langle A_1 G_k^{(3)}, G_m^{(3)}\rangle \\ &= \langle A_{3,FD}\mathbf{G}_k, \mathbf{G}_m\rangle,\end{aligned}$$

where $A_{3,FD}$ denotes the finite difference (FD) discrete Laplacian,

$$A_{3,FD} := A^{(1)} \otimes I^{(2)} \otimes I^{(3)} + I^{(1)} \otimes A^{(2)} \otimes I^{(3)} + I^{(1)} \otimes I^{(2)} \otimes A^{(3)},$$

with $I^{(\ell)}$ being the $N \times N$ identity matrix.

It is worth to note that the extension of Lemma 5.1 to the case of d-dimensional Laplacian,

$$\overline{a}_{km} = \langle A_d \mathbf{G}_k, \mathbf{G}_m \rangle,$$

leads to the similar d-term sum representation.

5.2 Nuclear potential and identity operators

We consider the nuclear (core) potential operator describing the Coulomb interaction of the electrons with the nuclei,

$$V_c(x) = -\sum_{\nu=1}^{M} \frac{Z_\nu}{\|x - a_\nu\|}, \quad Z_\nu > 0, \;\; a_\nu \in \mathbb{R}^3, \tag{5.8}$$

where M is the number of nuclei, and a_ν, Z_ν, represent the corresponding coordinates and charge numbers. Thus, the core potential for the molecule is represented by a tensor

$$\mathbf{P}_c = \sum_{\nu=1}^{M} Z_\nu \mathbf{P}_{c,\nu},$$

where $\mathbf{P}_{c,\nu}$ are the single Coulomb potentials shifted according to the coordinates of the corresponding nuclei. For the grid-based representation of the Newton potentials, $\mathbf{P}_{c,\nu}$, we return to the piecewise constant discretization on the equidistant tensor grid $\omega_{\mathbf{3},n}$, (4.2), introduced in §3, where, in general, the univariate grid size n can be noticeably smaller than the size N used for the piecewise linear discretization.

Remark 5.3 *It should be noted, that since we remain in the concept of global basis functions for the Galerkin approximation to the eigenvalue problem, the grid-based representation of these basis functions can be different in the calculation of the kinetic and potential parts in the Fock operator. The corresponding choice is the only controlled by the respective approximation error and by the numerical efficiency.*

For the core potential operator, V_c in (5.8), the entries of the respective Galerkin matrix, $V_G = \{\overline{v}_{km}\}$, are calculated (approximated) by the following tensor operation,

$$\overline{v}_{km} = \int_{\mathbb{R}^3} V_c(x) \overline{g}_k(x) \overline{g}_m(x) dx \approx \langle \mathbf{G}_k \odot \mathbf{G}_m, \mathbf{P}_c \rangle, \quad 1 \le k, m \le N_b, \tag{5.9}$$

where $\{\overline{g}_k\}$ denotes the piecewise constant representations to the respective Galerkin basis functions.

The error $\varepsilon > 0$ arising due to the separable approximation of the nuclear potential is controlled by the rank parameter $R_P = rank(\mathbf{P}_c)$. Now letting $rank(\mathbf{G}_m) = R_m$ implies that each matrix element is to be computed with linear complexity in n, $O(R_k R_m R_P\, n)$.

The almost exponential convergence of the rank approximation in R_P allows us the choice $R_P = O(|\log \varepsilon|)$.

Finally, we note that the Galerkin tensor representation of the identity operator leads to the following mass matrix, $S = \{\overline{s}_{km}\}$,

$$\overline{s}_{km} = \int_{\mathbb{R}^3} \overline{g}_k(x)\overline{g}_m(x)dx \approx \langle \mathbf{G}_k, \mathbf{G}_m \rangle, \quad 1 \le k, m \le N_b.$$

To conclude this section we note that the error bound $\|V_g - V_G\| \le Ch^2$ can be proven along the line of the discussion in [19].

6 Numerical results

6.1 Laplace operator in Gaussian basis

We consider the evaluation of a Galerkin matrix entry for the identity and Laplace operators,

$$\langle g, g \rangle = \int_{\mathbb{R}^3} g(x)^2 dx, \quad \langle -\Delta g, g \rangle = \int_{\mathbb{R}^3} \nabla g(x) \cdot \nabla g(x) dx, \quad g(x) = e^{-\alpha \|x\|^2}, \quad x \in \mathbb{R}^3,$$

for a single Gaussian with sufficiently large α and using large $N \times N \times N$ Cartesian grids. Functions are discretized according to (5.1) in the computational box $[-b, b]^3$, with $b = 14.6$ au ≈ 8 Å.

For a single Gaussian, we compare $\mathcal{J}_h$ computed as in Lemma 5.1 with the exact expression

$$\mathcal{J} = \int_{\mathbb{R}^3} \nabla g(x) \cdot \nabla g(x) dx = 3 J_1 \, J_{01}^2,$$

where

$$J_1 = 4\alpha^2 \int_{-\infty}^{\infty} x^2 e^{-2\alpha x^2} dx = \sqrt{\frac{\pi}{2}} \sqrt{\alpha}, \quad J_{01} = \int_{-\infty}^{\infty} e^{-\alpha x^2} dx = \frac{\sqrt{\pi}}{\sqrt{\alpha}}.$$

Table 6.1 shows the approximation error $|\mathcal{J} - \mathcal{J}_h|$ versus the grid size, where $\mathcal{J}_h$ is the grid-based evaluation of the matrix element on the corresponding grid, for $\alpha = 2500$, $4 \cdot 10^4$, and $1.2 \cdot 10^5$, which exceed the largest exponents α in the conventional Gaussian sets for hydrogen ($\alpha = 1777$), carbon ($\alpha = 6665$), oxygen ($\alpha = 11720$) and mercury ($\alpha = 10^5$) atoms. Computations confirm the results of Theorem 8.4 on the error bound, $O(h^2)$. It is easily seen that the errors reduce by a distinct factor of 4 for the grids corresponding to every next power of 2. Therefore, in spite of sharp "needles" of Gaussians due to large α, the Richardson extrapolation [29] (RE column) on a sequence of large grids provides a higher accuracy of the order $O(h^3) \div O(h^4)$.

In Table 6.1, the largest grid size $N = 2^{19} - 1$ corresponds to the computational box $\Omega \in \mathbb{R}^3$ with the huge number of entries of order $2^{57} \approx 10^{17}$. The corresponding mesh-size is of order $h \sim 10^{-5}$ Å. Computing times in MATLAB range from several milliseconds up to 1.2 sec for the largest grid.

Notice that the integral $\langle g, g \rangle = \int_{\mathbb{R}^3} e^{-2\alpha\|x\|^2} dx = J_{01}^3(\alpha)$ involved in the calculation of the mass-matrix S_g, is approximated with the same accuracy.

		$\alpha = 2.5 \cdot 10^3$		$\alpha = 4 \cdot 10^4$		$\alpha = 1.2 \cdot 10^5$	
p	N^3	$\lvert\mathcal{J} - \mathcal{J}_h\rvert$	RE	$\lvert\mathcal{J} - \mathcal{J}_h\rvert$	RE	$\lvert\mathcal{J} - \mathcal{J}_h\rvert$	RE
12	4095^3	0.0037	-	0.0058	-	0.025	-
13	8191^3	$9.3 \cdot 10^{-4}$	$1.0 \cdot 10^{-5}$	0.0034	0.0026	$2.4 \cdot 10^{-5}$	-
14	16383^3	$2.3 \cdot 10^{-4}$	$1.2 \cdot 10^{-6}$	$9.1 \cdot 10^{-4}$	$9.1 \cdot 10^{-5}$	0.0015	-
15	32767^3	$5.8 \cdot 10^{-5}$	$7.6 \cdot 10^{-8}$	$2.3 \cdot 10^{-4}$	$4.8 \cdot 10^{-6}$	$4.03 \cdot 10^{-4}$	$3.8 \cdot 10^{-5}$
16	65535^3	$1.4 \cdot 10^{-5}$	$4.7 \cdot 10^{-9}$	$5.8 \cdot 10^{-5}$	$3.0 \cdot 10^{-7}$	$1.0 \cdot 10^{-4}$	$1.6 \cdot 10^{-6}$
17	131071^3	$3.6 \cdot 10^{-5}$	$2.4 \cdot 10^{-10}$	$1.5 \cdot 10^{-5}$	$1.9 \cdot 10^{-8}$	$5.5 \cdot 10^{-5}$	$1.0 \cdot 10^{-7}$
18	262143^3	$9.1 \cdot 10^{-7}$	$3.1 \cdot 10^{-11}$	$3.6 \cdot 10^{-6}$	$1.2 \cdot 10^{-9}$	$6.4 \cdot 10^{-6}$	$6.5 \cdot 10^{-9}$
19	524287^3	$2.2 \cdot 10^{-7}$	$5.4 \cdot 10^{-13}$	$9.1 \cdot 10^{-7}$	$7.3 \cdot 10^{-11}$	$1.6 \cdot 10^{-6}$	$4.0 \cdot 10^{-10}$

Table 6.1: Approximation error $|\mathcal{J} - \mathcal{J}_h|$ for the grid-based evaluation of the Laplacian Galerkin matrix entry for a Gaussian $g(x) = e^{-\alpha\|x\|^2}$, $x \in \mathbb{R}^3$, $N = 2^p - 1$.

6.2 Grid-based Schrödinger equation for the hydrogen atom

In this section, we verify the proposed algorithms by the grid-based solution of the Hartree-Fock equation for the hydrogen atom,

$$\mathcal{H}\psi = \lambda\psi, \quad \mathcal{H} = -\frac{1}{2}\Delta + \frac{1}{\|x\|}, \quad x \in \mathbb{R}^3, \tag{6.1}$$

which has an exact solution $\psi = e^{-\|x\|} / \sqrt{\pi}$, $\lambda = -1/2$.

Example 1. Consider the traditional expansion of the solution using the ten s-type primitive Gaussian functions from the cc-pV6Z basis set [21, 23],

$$\psi(x) \approx \sum_{k=1}^{N_b} c_k \varphi_k(x), \quad N_b = 10, \ x \in \mathbb{R}^3,$$

which leads to the Galerkin equation (2.10) corresponding to (6.1), with

$$F = \langle \mathcal{H}\overline{g}_k, \overline{g}_m \rangle := -\frac{1}{2}\langle \Delta\overline{g}_k, \overline{g}_m \rangle + \langle \frac{1}{\|x\|}\overline{g}_k, \overline{g}_m \rangle, \quad k, m = 1, \dots N_b,$$

with respect to the Galerkin basis $\{\overline{g}_k\}$. We choose the appropriate size of the computational box (4.1) as $b \approx 8$ Å and discretize $\{\overline{g}_k\}$ using $N \times N \times N$ Cartesian grid, obtaining the canonical rank-1 tensor representation $\mathbf{G}_k$ of the basis functions. Then, the kinetic energy and the nuclear potential parts of the Fock operator are computed by (5.4), (5.9) from §5.

Table 6.2, line (1), presents numerical errors in energy, $|\lambda - \lambda_h|$, of the grid-based calculations using the cc-pV6Z basis set of $N_b = 10$ Gaussians generated by MOLPRO [16], providing an accuracy of order $\sim 10^{-6}$. Notice that this accuracy is achieved already at the grid-size $N = 8192$, hence, further grid refinement does not improve the results.

Example 2. Here we study the effect of basis optimization by adding an auxiliary basis function to the Gaussian basis set from the previous example, thus increasing the number of basis functions to $N_b = 11$. The second line (2) in Table 6.2 shows improvement of accuracies for the basis augmented by a rank-1 approximation to the Slater function given

N^3	512^3	1024^3	2048^3	4096^3	8192^3	16384^3	32768^3
(1) $\|\lambda - \lambda_h\|$	0.0015	$4.1 \cdot 10^{-4}$	$1.0 \cdot 10^{-4}$	$2.7 \cdot 10^{-5}$	$7.5 \cdot 10^{-6}$	$2.4 \cdot 10^{-6}$	$1.0 \cdot 10^{-6}$
(2) $\|\lambda - \lambda_h\|$	$9.7 \cdot 10^{-5}$	$1.5 \cdot 10^{-5}$	$7.2 \cdot 10^{-6}$	$2.7 \cdot 10^{-6}$	$1.1 \cdot 10^{-6}$	$8.0 \cdot 10^{-7}$	$7.8 \cdot 10^{-7}$
(3) $\|\lambda - \lambda_h\|$	$4.3 \cdot 10^{-4}$	$1.0 \cdot 10^{-4}$	$2.7 \cdot 10^{-5}$	$6.8 \cdot 10^{-6}$	$1.7 \cdot 10^{-6}$	$4.3 \cdot 10^{-7}$	-

Table 6.2: Examples 5.1 – 5.3 for hydrogen atom: $|\lambda - \lambda_h|$ vs. grid size N^3, for (1) the discretized basis of $N_b = 10$ Gaussians, (2) 11 basis functions consisting of Gaussians augmented by a rank-1 function φ_0, (3) discretized single Slater function of rank R_b.

N^3	512^3	1024^3	2048^3	4096^3	8192^3	16384^3	32768^3
(1): RE	-	$5.0 \cdot 10^{-5}$	$5.1 \cdot 10^{-6}$	$5.3 \cdot 10^{-7}$	$7.8 \cdot 10^{-7}$	$7.4 \cdot 10^{-7}$	$7.6 \cdot 10^{-7}$
(3): RE	-	$1.0 \cdot 10^{-6}$	$2.3 \cdot 10^{-7}$	$1.9 \cdot 10^{-8}$	$1.7 \cdot 10^{-8}$	$1.5 \cdot 10^{-8}$	-

Table 6.3: The Richardson extrapolation (RE) for Examples 5.1 and 5.3.

by the grid representation of $\varphi_0 = e^{-(|x_1|+|x_2|+|x_3|)}$. Augmenting by a piecewise linear hat function of the type ξ_i centered at the origin gives similar results as for φ_0.

Example 3. Here we present computations with the controlled accuracy using a single rank-R_b basis function generated by the sinc-approximation to the Slater function. Using the Laplace transform,

$$G(\rho) = e^{-2\sqrt{\alpha\rho}} = \frac{\sqrt{\alpha}}{\sqrt{\pi}} \int_0^\infty \tau^{-3/2} exp(-\alpha/\tau - \rho\tau) d\tau,$$

the Slater function can be represented as a rank-R canonical tensor by computing the sinc-quadrature decomposition [13], and setting $\rho = x_1^2 + x_2^2 + x_3^2$,

$$G(\rho) \approx \sum_{k=-L}^{L} \frac{\sqrt{\alpha}}{\sqrt{\pi}} w_k \tau_k^{-3/2} exp(-\alpha/\tau_k) \prod_{\ell=1}^{3} exp(-\tau_k x_\ell^2),$$

where $\tau_k = e^{kh_L}$, $w_k = h_L \tau_k$, $h_L = C_0 \log L/L$. The accuracy of the approximation, $\varepsilon > 0$, is controlled by choosing the number of quadrature points L. In this example, we have only one basis function in a set, an approximate Slater function, but represented by the canonical tensor of rank $R_b \leq 2L + 1$. Thus, each of the matrices A_G computed by (5.7), and V_G are of size 1×1. Table 6.2 (3) shows accuracy of the solution to the Hartree-Fock equation for the hydrogen atom, using one approximate Slater basis function.

Table 6.3 presents the Richardson extrapolation for Examples 1 and 3. Due to noticable convergence rate of order $O(h^2)$ the Richardson extrapolation gives further improvement of the accuracy up to $O(h^3)$. It is seen in Table 6.3, line (3), that the Richardson extrapolation for the results of Example 3 gives accuracy of the order 10^{-7} beginning from the grid size 4096. Note that with the choice $L = 60$, the accuracies are one order of magnitude better than those obtained for the standard gaussian basis set in Example 1.

6.3 Numerics for the grid-based core Hamiltonian matrix

Tables 6.4 – 6.8 present the numerical examples of the grid-based approximation to the Galerkin matrices for the Laplace, A_G, and nuclear potential, V_G, operators using (5.4) and (5.9) from §5.1 and §5.2 for the molecules HF (hydrogen fluoride), H_2O, NH_3, CH_4, H_2O_2, N_2H_4 and C_2H_5OH. The same computational box $[-b, b]^3$ with $b = 14.6$ au is used for all considered molecules. Mesh size of the $N \times N \times N$ Cartesian grid ranges from $h = 0.0036$ au (atomic units) corresponding to $N = 8192$, up to $h = 2.2 \cdot 10^{-4}$ au for $N = 131072$.

Figure 6.1 shows the structure of C_2H_5OH molecule. In our calculations the atomic nuclei are placed arbitrarily with respect to the grid points of the uniform 3D Cartesian grid.

The maximum computational time for $N^3 = 131072^3$ is of the order of hundred seconds in MATLAB for A_G, and hundred minutes for V_G. For $N^3 = 8192^3$ computations are in the range of several seconds for both A_G and V_G.

Tables 6.4 – 6.8 show the relative Frobenius norm of the differences in the corresponding Galerkin matrix entries for the Laplace $Er(A_G)$ and nuclear potential $Er(V_G)$ operators, where

$$Er(A_G) = \frac{\|A_g - A_G\|}{\|A_g\|}, \quad Er(V_G) = \frac{\|V_g - V_G\|}{\|V_g\|}.$$

The quadratic convergence of both quantities along the line of dyadic grid refinement is in good agreement with the theoretical error estimates in §8. Therefore the employment of the Richardson approximation providing the error

$$E_{Ri,2h,h} = Er\left(\frac{4 * V_{G,h} - V_{G,2h}}{3}\right)$$

gives further improvement of the accuracy up to order of $O(h^4)$ for the Laplace operator. The "RE" lines in Tables 6.4 – 6.8 demonstrate the results of the Richardson extrapolation applied to corresponding quantities at the adjacent grids. Lines $|a_{11} - \overline{a}_{11}|$ and $|v_{11} - \overline{v}_{11}|$ show the absolute accuracy of calculating the first (largest) components of the matrices A_g and V_g, respectively.

Figure 6.2 shows absolute error for the grid-based computation of matrix entries for the Laplace (left) and nuclear potential (right) operators corresponding to H_2O, with respect to the matrices from MOLPRO. The Richardson extrapolation is applied to grids of size $2^{15 \cdot 3}$ and $2^{16 \cdot 3}$. Note, that the values of the largest entries of these matrices are $a_{11} = 17580$ and $v_{11} = 1385$, respectively. We observe the relative computation errors of order of 10^{-7} using the efficient tensor methods on uniform 3D Cartesian grids.

6.4 Grid-based numerical solution of the Hartree-Fock equation

Here, we sketch the general scheme for the multilevel numerical solution of the Hartree-Fock equation by tensor-structured methods introduced in [3, 2]. The main difference from the standart numerical approach is that it does not use the two-electron integrals, and instead the Coulomb and exchange operators are computed "on the fly" during the DIIS iterations.

Figure 6.3, (see [3]) shows the flow-chart of the "black-box" 3D solver for the Hartree-Fock equation. Here $N = N_0 \cdot 2^p$ is the univariate size of the $N \times N \times N$ 3D Cartesian grid, where N_0 is the size of the coarsest grid, and p indicates the grid level. k is the iteration number, and k_0 (usually $k_0 = 4$) indicates the grid level to begin the DIIS [25] scheme.

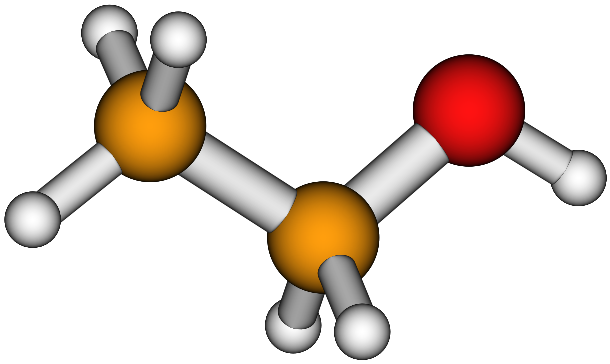

Figure 6.1: The molecular structure of ethanol (C_2H_5OH). Figure is generated using the MOLDEN program [24].

p	13	14	15	16	17
$N^3 = 2^{3p}$	8192^3	16384^3	32768^3	65536^3	131072^3
$Er(A_G)$	0.032	0.0083	0.0021	$5.2 \cdot 10^{-4}$	$1.3 \cdot 10^{-4}$
RE	-	$4.0 \cdot 10^{-4}$	$3.3 \cdot 10^{-5}$	$6.0 \cdot 10^{-6}$	$5.0 \cdot 10^{-8}$
$\lvert a_{11} - \overline{a}_{11} \rvert$	208	52	13	3.3	0.82
RE	11	0.72	0.045	0.0028	$1.3 \cdot 10^{-4}$
$Er(V_G)$	0.024	0.0083	0.0011	$3.1 \cdot 10^{-4}$	
RE	-	0.0031	0.0013	$5.9 \cdot 10^{-5}$	
$\lvert v_{11} - \overline{v}_{11} \rvert$	14	5.4	0.8	0.3	
RE	11	0.72	0.045	0.0028	

Table 6.4: Ethanol (C_2H_5OH): accuracy of the Galerkin matrices corresponding to the Laplace, $Er(A_G)$, and the nuclear potential operators, $Er(V_G)$, using the discretized basis of 123 primitive Cartesian Gaussians (from the cc-pVDZ set [22, 23]).

p	13	14	15	16	17
$N^3 = 2^{3p}$	8192^3	16384^3	32768^3	65536^3	131072^3
$Er(A_G)$	0.027	0.0069	0.0017	$4.3 \cdot 10^{-4}$	$1.08 \cdot 10^{-4}$
RE		$1.08 \cdot 10^{-4}$	$3.0 \cdot 10^{-5}$	$1.3 \cdot 10^{-5}$	$3.6 \cdot 10^{-8}$
$\lvert a_{11} - \overline{a}_{11,h} \rvert$	382	97	24	6	1.5
RE		2	0.3	0.0	0.0
$Er(V_G)$	0.022	0.0064	0.001	$3.6 \cdot 10^{-4}$	$8.9 \cdot 10^{-5}$
RE		0.0012	$8.0 \cdot 10^{-4}$	$1.5 \cdot 10^{-4}$	$9.0 \cdot 10^{-8}$
$\lvert v_{11} - \overline{v}_{11,h} \rvert$	29	8.5	1.4	0,48	0.11
RE		1.6	0.99	0.18	$3.9 \cdot 10^{-3}$

Table 6.5: Hydrazine (N_2H_4): accuracy of the Laplace-Galerkin matrix, $Er(A_G)$, and the nuclear potential operators, $Er(V_G)$, using the discretized basis of 82 primitive Cartesian Gaussians (from the cc-pVDZ set [22, 23]). $a_{11} = 13569$, $v_{11} = 1063$.

p	13	14	15	16	17	18
$N^3 = 2^{3p}$	8192^3	16384^3	32768^3	65536^3	131072^3	262144^3
$Er(A_G)$		0.0083	0.0021	$5.2 \cdot 10^{-4}$	$1.3 \cdot 10^{-4}$	$3.2 \cdot 10^{-5}$
RE	-		$3.3 \cdot 10^{-5}$	$6.0 \cdot 10^{-6}$	$5.0 \cdot 10^{-8}$	$2.0 \cdot 10^{-9}$
$\lvert a_{11} - \overline{a}_{11,h} \rvert$		162	40	10	2.55	0.6
RE	-		0.6	0.0154	$9.3 \cdot 10^{-4}$	$6.6 \cdot 10^{-5}$
$Er(V_G)$	0,025	0.0066	0.0025	$2.9 \cdot 10^{-4}$	$8.75 \cdot 10^{-5}$	
RE		$4.6 \cdot 10^{-4}$	0.001	$4.0 \cdot 10^{-4}$	$2.0 \cdot 10^{-5}$	
$\lvert v_{11} - \overline{v}_{11,h} \rvert$	41	10.9	4.2	0.49	0.144	
RE	-	0.8	1.9	0.7	0.028	

Table 6.6: Hydrogen peroxide (H_2O_2): accuracy of the Laplace-Galerkin matrix, $Er(A_G)$, and the nuclear potential operators, $Er(V_G)$, using the discretized basis of 68 primitive Cartesian gaussians (from the cc-pVDZ set [22, 23]). $a_{11} = 17580$, $v_{11} = 1385$.

p	13	14	15	16	17
$N^3 = 2^{3p}$	8192^3	16384^3	32768^3	65536^3	131072^3
h(in au)	0.0036	0.0018	$8.9 \cdot 10^{-4}$	$4.4 \cdot 10^{-4}$	$2.2 \cdot 10^{-4}$
$Er(A_G)$	0.02	0.052	0.0013	$3.2 \cdot 10^{-4}$	$8 \cdot 10^{-5}$
RE	-	$2.6 \cdot 10^{-4}$	0	$2.0 \cdot 10^{-6}$	$1.7 \cdot 10^{-8}$
$Er(V_G)$	0.012	0.0029	$7.0 \cdot 10^{-4}$	$1.7 \cdot 10^{-4}$	$4.3 \cdot 10^{-5}$
RE	-	$2.6 \cdot 10^{-4}$	$2.0 \cdot 10^{-5}$	$3.0 \cdot 10^{-6}$	$1.2 \cdot 10^{-7}$

Table 6.7: Methane (CH_4): accuracy of the Galerkin matrices corresponding to the Laplace, $Er(A_G)$, and the nuclear potential operators, $Er(V_G)$, using the discretized basis of 55 primitive Cartesian Gaussians (from the cc-pVDZ set [22, 23]).

p	13	14	15	16	17
$N^3 = 2^{3p}$	8192^3	16384^3	32768^3	65536^3	131072^3
$Er(A_G)$	0.0439	0.0112	0.0028	$7.0 \cdot 10^{-4}$	$1.7 \cdot 10^{-4}$
RE		$3.0 \cdot 10^{-4}$	0.0	0.0	$8 \cdot 10^{-8}$
$\lvert a_{11} - \overline{a}_{11,h} \rvert$	999	255	64	16	4
RE		7	0.3	0.0	0.0
$Er(V_G)$	0.029	0.0065	0.0016	$4.0 \cdot 10^{-4}$	$1.18 \cdot 10^{-4}$
RE		0.0012	$3.3 \cdot 10^{-5}$	0.0	$2.3 \cdot 10^{-5}$

Table 6.8: Hydrogen fluoride (HF): accuracy of the Laplace-Galerkin matrix, $Er(A_G)$, and the nuclear potential operators, $Er(V_G)$, using the discretized basis of 34 primitive Cartesian Gaussians (from the cc-pVDZ set [22, 23]). $a_{11} = 22065$

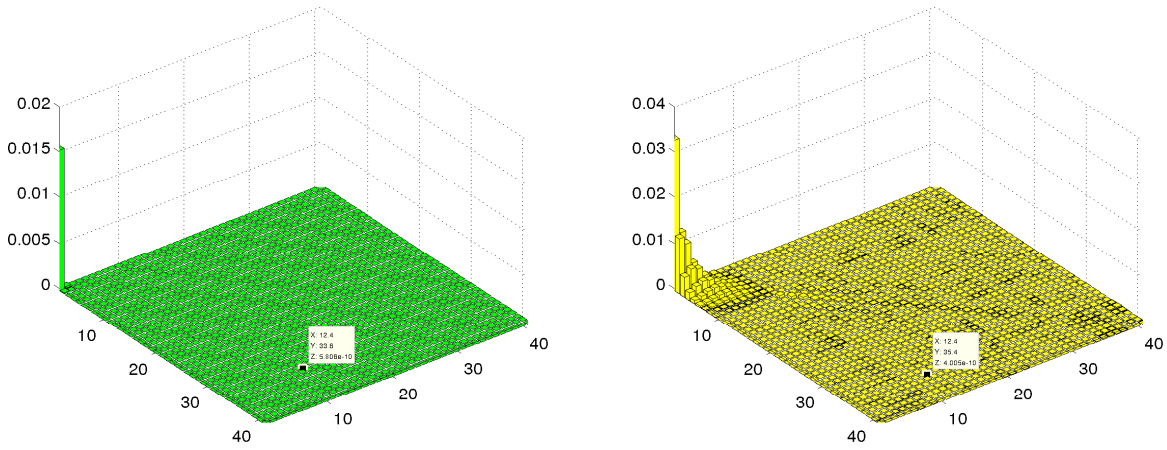

Figure 6.2: Absolute error of grid-based computation of matrix entries for the Laplace (left) and nuclear potential (right) operators for H_2O, compared to data from MOLPRO. The Richardson extrapolation is applied on grids 2^{45} and 2^{48}.

First, the (solution independent) core Hamiltonian part, H_0, of the Fock operator is computed as discussed above for a given basis set. Note, that the size of the 3D Cartesian grids used at this step may be much different (larger) from those used further in calculations of the Hartree and exchange potentials.

Then, the EVP (2.10) is solved with the zero initial guess, $J_{N_0}(C) = 0$, $K_{N_0}(C) = 0$. The DIIS iteration on N^3 3D Cartesian grid, is started on a coarse grid, say, with $N_0 = 64$, and proceed using the dyadic grid refinement up to $N^3 = 8192^3$ or $N^3 = 16384^3$. The mesh size at fine grids is of the order $h \approx 9 \cdot 10^{-4}$ $\overset{\circ}{A}$. At every iteration step, the Coulomb and exchange parts of the Fock matrix F are updated by the tensor-structured computations in $O(N \log N)$ complexity. A grid dependent termination criterion is used for switching iterations to the next level of grid refinement. For example, as the termination criterion, we control the norms of the differences for the virtual orbitals taken as the residual over subsequent iterations.

The multilevel strategy provides fast and robust convergence of the SCF DIIS iteration in spite of zero initial guess for $J_{N_0}(C)$, $K_{N_0}(C)$, since the results on the coarse grids serve as a good initial guess for iterations on time consuming finer grids. The improved asymptotical approximation $O(h^3)$ is obtained due to the Richardson extrapolation over a sequence of grids [29].

Figure 6.4 shows iterations history of the solver for NH_3 molecule. Red line shows the convergence of the residual, the blue line is the difference of the first (largest by absolute value) eigenvalue from the value from MOLPRO.

7 Conclusions

Here we present a fast and accurate grid-based method for calculation of the Galerkin matrices for the Laplace and nuclear potential parts in the Fock operator. It is based on tensor

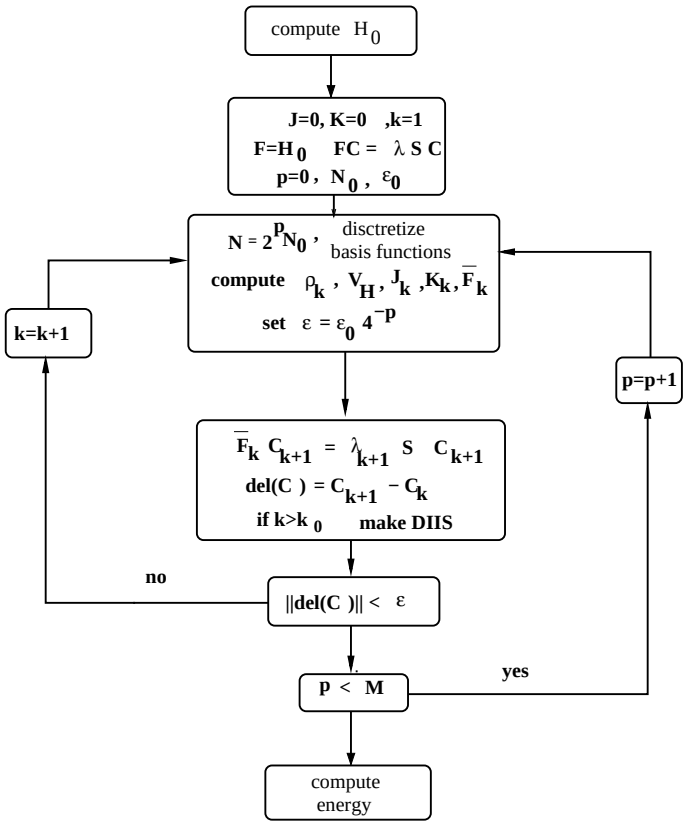

Figure 6.3: Flow-chart of the "black-box" Hartree-Fock solver.

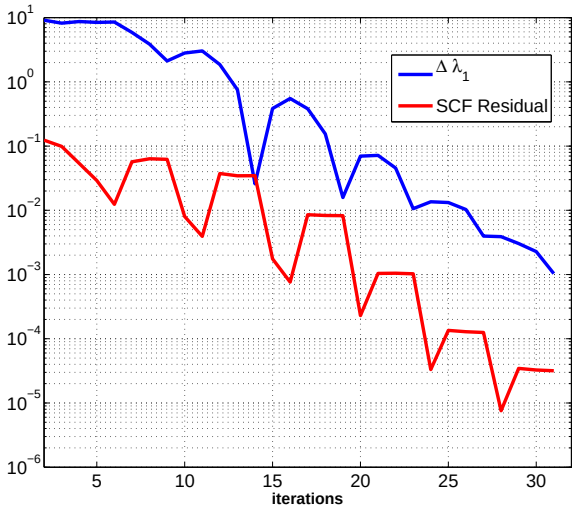

Figure 6.4: Convergence with respect to iterations of the Hartree-Fock solver. NH_3 molecule, the largest grid size $N^3 = 4096^3$.

operations of complexity $O(N)$, applied to the generic set of basis functions with low separation rank, and discretized on fine $N \times N \times N$ Cartesian grids thus ensuring high precision. The discretization error estimate of order $O(h^2)$ is proven. The Richardson extrapolation is shown to provide the improved approximation of order $O(h^3)$-$O(h^4)$. The efficiency and accuracy of the approach is demonstrated by numerical tests on some moderate size compact organic molecules.

Note that in the grid-based evaluation of the Fock operator we use two levels of basis functions. The Galerkin scheme for the Hartree-Fock eigenvalue problem is treated in the AO global basis, while the global basis functions are represented on the grid, using the piecewise linear or piecewise constant finite elements of the second representation level. Such separation provides the choice of optimal grid sizes in computation of different parts of the Fock operator, being controlled only by the respective approximation error.

The reported results for the core Hamiltonian and already mentioned method for the Coulomb and exchange matrices provide an approach to the numerical solution of the Hartree-Fock equation by efficient recomputation of the Fock matrix "on the fly" [3] in the case of multiply changing and rather general basis sets specified, in particular, by their grid representation. These arise, for example, in the potential energy surface calculations in molecular dynamics. Other possible advantageous application areas include semiperiodic systems [27, 28] and the grid-based evaluation of the two-electron integrals tensor in Hartree-Fock and post Hartree-Fock calculations.

Acknowledgements. The authors are grateful to Prof. Dr. Reinhold Schneider (TU Berlin) and Dr. Heinz-Juergen Flad (TU Berlin) for valuable discussions and useful comments.

8 Appendix 1: error control

In this section we prove the asymptotic estimate, $O(h^2)$, for the numerical errors $\|S_g - S_G\|$, $\|A_g - A_G\|$ and $\|V_g - V_G\|$ in the max- and Frobenius norms effected by the piecewise linear interpolation of the initial basis functions $\mathbf{I}_1 : g_k(x) \to \overline{g}_k(x)$. The numerical illustrations for these results are presented in Section 6.

First, consider the approximation error in the Galerkin stiffness matrix, $\|A_g - A_G\|$, corresponding to the Laplacian. Recall, that in this case $\overline{g}_k^{(\ell)} = I_1 g_k^{(\ell)}$, $\ell = 1, ..., 3$. We begin from some auxiliary error bounds in $1D$ case. Though these estimates are apparently known in the FEM community, for the convenience we present complete proofs. Denote $\Omega = (-b, b)$, and $\overline{u} = I_1 u$.

Lemma 8.1 *Let $u \in H_0^1(\Omega) \cap H^2(\Omega)$, then*

$$|\langle u', u' \rangle - \langle (I_1 u)', (I_1 u)' \rangle| \leq C h^2 \|u''\|_0^2, \tag{8.1}$$

$$|\|u\|_0^2 - \|I_1 u\|_0^2| \leq C h^2 \|u''\|_0 \|u\|_0, \tag{8.2}$$

where C is independent of h and u.

Proof. Recall the standard FEM error bounds [30],

$$\|u - I_1 u\|_0 \le Ch^2 \|u''\|_0, \quad \|u' - (I_1 u)'\|_0 \le Ch\|u''\|_0. \tag{8.3}$$

It is easy to check the identity

$$\langle a, a\rangle - \langle b, b\rangle = -\langle a - b, a - b\rangle + 2\langle a, a - b\rangle \quad \forall a, b \in L^2(\Omega). \tag{8.4}$$

Plugging $a = u'$, $b = (I_1 u)'$ in (8.4), taking into account the equation

$$\langle u', (u - I_1 u)'\rangle = -\langle u'', u - I_1 u\rangle,$$

and bounds (8.3), we arrive at (8.1).

Now replacing in (8.4) $a = u$, $b = I_1 u$, and making use of (8.3) yields (8.2). ∎

Lemma 8.2 *Let $u, v \in H_0^1(\Omega) \cap H^2(\Omega)$, then*

$$|\langle u', v'\rangle - \langle (I_1 u)', (I_1 v)'\rangle| \le Ch^2 \|u''\|_0 \|v''\|_0,$$
$$|\langle u, v\rangle - \langle I_1 u, I_1 v\rangle| \le Ch^2 \|u''\|_0 \|v''\|_0,$$

where C is independent of h and u.

Proof. To prove the first assertion, we apply Lemma 8.1, (8.1), to the identity

$$\langle a, b\rangle - \langle \overline{a}, \overline{b}\rangle = \langle a, a\rangle - \langle \overline{a}, \overline{a}\rangle + \langle b, b\rangle - \langle \overline{b}, \overline{b}\rangle - \langle a - b, a - b\rangle - \langle \overline{a} - \overline{b}, \overline{a} - \overline{b}\rangle,$$

where $a = u'$, $b = v'$, $\overline{a} = (I_1 u)'$, $\overline{b} = (I_1 v)'$. The second estimate follows from (8.2) by substitution $a = u$, $b = v$, $\overline{a} = I_1 u$, $\overline{b} = I_1 v$. ∎

Next, we prove the simple technical lemma.

Lemma 8.3 *Given $d \in \mathbb{N}$, and $a_\ell, \overline{a}_\ell \in \mathbb{R}$, such that for some constants $C, E > 0$ we have $|a_\ell - \overline{a}_\ell| \le E$, $|a_\ell|, |\overline{a}_\ell| \le C$ for $\ell = 1, 2, \dots d$. Then it holds*

$$\left| \prod_{\ell=1}^{d} a_\ell - \prod_{\ell=1}^{d} \overline{a}_\ell \right| \le dEC^{d-1}.$$

Proof. The result can be proven by induction in d. Introduce the notation

$$E(k) = \max_{1 \le n \le d+1-k} \left\{ \left| \prod_{\ell=n}^{n+k-1} a_\ell - \prod_{\ell=n}^{n+k-1} \overline{a}_\ell \right| \right\}, \quad k = 1, \dots, d,$$

and prove that $E(k) \le kEC^{k-1}$. Notice that by assumptions, $E(1) \le E$, and $E(d)$ coincides with the target quantity. Now assuming that for the dimension $d - 1$ the estimate is valid, we get

$$\begin{aligned} \left| \prod_{\ell=1}^{d} a_\ell - \prod_{\ell=1}^{d} \overline{a}_\ell \right| &= |a_1(a_2 \cdots a_d - \overline{a}_2 \cdots \overline{a}_d) + (a_1 - \overline{a}_1)\overline{a}_2 \cdots \overline{a}_d| \\ &\le CE(d-1) + E(1)C^{d-1} \\ &= C(d-1)EC^{d-2} + EC^{d-1} \\ &= dEC^{d-1}, \end{aligned}$$

which completes our proof. ∎

We further denote by $\nabla_{(d)}$ the d-dimensional gradient operator. Now we are in a position to prove the basic approximation result.

Theorem 8.4 *(d-dimensional approximation). Let* $u(x) = \prod_{\ell=1}^{d} u_\ell(x_\ell)$, $v(x) = \prod_{\ell=1}^{d} v_\ell(x_\ell)$, *where* $u_\ell, v_\ell \in H_0^1(\Omega) \cap H^2(\Omega)$, $\ell = 1, \ldots, d$, *then*

$$\left|\langle \nabla_{(d)} u, \nabla_{(d)} v\rangle - \langle \nabla_{(d)} \mathbf{I}_1 u, \nabla_{(d)} \mathbf{I}_1 v\rangle\right| \le d C_0^{d-1}(E_1 + E_0(d-1)C_1/C_0), \tag{8.5}$$

$$|\langle u, v\rangle - \langle \mathbf{I}_1 u, \mathbf{I}_1 v\rangle| \le d^2 E_0 C_0^{d-1}, \tag{8.6}$$

where $C_0 = \max_\ell\{|\langle u_\ell, v_\ell\rangle|, |\langle I_1 u_\ell, I_1 v_\ell\rangle|\}$, $C_1 = \max_\ell\{|\langle u'_\ell, v'_\ell\rangle|, |\langle (I_1 u_\ell)', (I_1 v_\ell)'\rangle|\}$, $E_0 = \max_\ell\{|\langle u_\ell, v_\ell\rangle - \langle I_1 u_\ell, I_1 v_\ell\rangle|\}$, *and* $E_1 = \max_\ell\{|\langle u'_\ell, v'_\ell\rangle - \langle (I_1 u_\ell)', (I_1 v_\ell)'\rangle|\}$.

Proof. The result follows by Lemmas 8.2, 8.3. In fact, it is easy to see that

$$\begin{aligned}
& \langle \nabla_{(d)} u, \nabla_{(d)} v\rangle - \langle \nabla_{(d)} \mathbf{I}_1 u, \nabla_{(d)} \mathbf{I}_1 v\rangle \\
= & \sum_{k=1}^{d} \left[\langle u'_k, v'_k\rangle \prod_{\ell=1,\ell\neq k}^{d} \langle u_\ell, v_\ell\rangle - \langle (I_1 u_k)', (I_1 v_k)'\rangle \prod_{\ell=1,\ell\neq k}^{d} \langle I_1 u_\ell, I_1 v_\ell\rangle \right] \\
= & \sum_{k=1}^{d} \langle u'_k, v'_k\rangle \left(\prod_{\ell=1,\ell\neq k}^{d} \langle u_\ell, v_\ell\rangle - \prod_{\ell=1,\ell\neq k}^{d} \langle I_1 u_\ell, I_1 v_\ell\rangle \right) \\
+ & \sum_{k=1}^{d} (\langle u'_k, v'_k\rangle - \langle (I_1 u_k)', (I_1 v_k)'\rangle) \prod_{\ell=1,\ell\neq k}^{d} \langle I_1 u_\ell, I_1 v_\ell\rangle \\
\le & \; d(C_1 E_0 (d-1) C_0^{d-2} + E_1 C_0^{d-1}),
\end{aligned}$$

which proves the first assertion by applying Lemmas 8.2 and 8.3 with respective notations. The second assertion is proven in a similar way. ∎

In the following, we assume without loss of generality that $supp(g_k) = \Omega$, $k = 1, ..., N_b$.

Corollary 8.5 *Let* $d = 3$ *and the separable basis set* $\{g_k\}$ *satisfy the conditions of Theorem 8.4. Then the error estimates hold:*

$$\|A_g - A_G\|_\infty \le Ch^2, \quad \|S_g - S_G\|_\infty \le Ch^2. \tag{8.7}$$

Proof. Under the assumptions of Theorem 8.4, we have $E_0 = O(h^2)$, and $E_1 = O(h^2)$. Now setting in Theorem 8.4 $d = 3$, and denoting $u = g_k$, $v = g_m$, one derives from (8.5) the first estimate in (8.7),

$$\|A_g - A_G\|_\infty = \max_{k,m} \|a_{km} - \overline{a}_{km}\| \le Ch^2.$$

Similarly, (8.6) proves the second bound in (8.7). ∎

The above estimates are confirmed by the numerical illustrations in §6.

9 Appendix 2

For the readers convenience, Table 9.1 presents the nuclear coordinates used in computations of the core Hamiltonian for the molecules considered in this study: C_2H_5OH, N_2H_4, H_2O_2, CH_4, NH_3, H_2O and HF.

References

[1] B.N. Khoromskij and V. Khoromskaia. *Multigrid tensor approximation of function related multi-dimensional arrays.* SIAM J. Sci. Comp. 31(4) (2009) 3002-3026.

[2] B.N. Khoromskij, V. Khoromskaia, and H.-J. Flad. *Numerical Solution of the Hartree-Fock Equation in Multilevel Tensor-structured Format.* SIAM J. Sci. Comp. 33(1) (2011) 45-65.

[3] V. Khoromskaia. *Numerical Solution of the Hartree-Fock Equation by Multilevel Tensor-structured methods.* PhD thesis, TU Berlin, 2010.

[4] R.J. Harrison, G.I. Fann, T. Yanai, Z. Gan, and G. Beylkin. *Multiresolution quantum chemistry: Basic theory and initial applications.* J. of Chem. Phys. 121(23) (2004) 11587-11598.

[5] T. Yanai, G.I. Fann, Z. Gan, R.J. Harrison, G. Beylkin. *Multiresolution quantum chemistry in multiwavelet bases: Analytic derivatives for Hartree-Fock and density functional theory.* J. Chem. Phys. 121 (2004) 2866.

[6] J. Jusélius and D. Sundholm. *Parallel implementation of a direct method for calculating electrostatic potentials.* J. Chem. Phys. 126 (2007) 094101.

[7] D. R. Hartree. *The Calculation of Atomic Structure*, Wiley, New York, 1957.

[8] Ch. Froese Fischer. *The Hartree-Fock Method for Atoms — A Numerical Approach*, Wiley, New York, 1977.

[9] D. Andrae and J. Hinze. *Numerical Electronic Structure Calculations for Atoms. I. Generalized Variable Transformation and Nonrelativistic Calculations*, Int. J. Quantum Chem. 63 (1997) 65–91.

[10] L. Laaksonen, P. Pyykkö and D. Sundholm. *Fully numerical Hartree-Fock methods for molecules*, Comput. Phys. Rep. 4 (1986) 313–344.

[11] E. A. McCullough, Jr. *Numerical Hartree-Fock methods for molecules*, in P. v. R. Schleyer et al. (eds.), Encyclopedia of Computational Chemistry (Vol. 3), Wiley, Chichester, (1998) 1941–1947.

[12] M. Barrault, E. Cancès, W. Hager, and C. Le Bris. *Multilevel domain decomposition for electronic structure calculations.* J. Comp. Phys. 222 (2007) 86–109.

[13] B.N. Khoromskij. *Introduction to Tensor Numerical Methods in Scientific Computing.* Lecture Notes, University Zuerich, Preprint 06-2011, (2011) 1–238.

[14] B.N. Khoromskij. *$O(d \log N)$-Quantics Approximation of N-d Tensors in High-Dimensional Numerical Modeling.* Constr. Approx. 34 (2011) 257–280.

[15] C. Bertoglio, and B.N. Khoromskij. *Low-rank quadrature-based tensor approximation of the Galerkin projected Newton/Yukawa kernels.* Comp. Phys. Comm. 183(4) (2012) 904–912.

[16] H.-J. Werner, P.J. Knowles, et al. MOLPRO version 2010.1, A Package of Ab-Initio Programs for Electronic Structure Calculations.

[17] T. Helgaker, P. Jørgensen, and J. Olsen. *Molecular Electronic-Structure Theory.* Wiley, New York, 1999.

[18] C. Le Bris. *Computational chemistry from the perspective of numerical analysis.* Acta Num. (2005), 363 - 444.

[19] B.N. Khoromskij. *Fast and Accurate Tensor Approximation of a Multivariate Convolution with Linear Scaling in Dimension.* J. Comp. Appl. Math. 234 (2010) 3122-3139.

[20] V. Khoromskaia. *Computation of the Hartree-Fock Exchange in the Tensor-structured Format.* Comp. Meth. App. Math., 10(2) (2010) 204–218.

[21] K. A. Peterson, D. E. Woon and T. H. Dunning, Jr. *Benchmark calculations with correlated molecular wave functions. IV. The classical barrier height of the H + H_2 → H_2 + H reaction*, J. Chem. Phys. 100 (1994) 7410–7415.

[22] T. H. Dunning, Jr. *Gaussian basis sets for use in correlated molecular calculations. I. The atoms boron through neon and hydrogen*, J. Chem. Phys. 90 (1989) 1007–1023.

[23] K. L. Schuchardt, B. T. Didier, T. Elsethagen, L. Sun, V. Gurumoorthi, J. Chase, J. Li, and T. L. Windus. *Basis Set Exchange: A Community Database for Computational Sciences*, J. Chem. Inf. Model. 47 (2007) 1045–1052.

[24] G.Schaftenaar and J.H. Noordik. Molden: a pre- and post-processing program for molecular and electronic structures. J. Comput.-Aided Mol. Design, 14 (2000) 123-134.

[25] P. Pulay. *Improved SCF convergence acceleration.* J. Comp. Chem. 3 (1982) 556–560.

[26] T. G. Kolda and B. W. Bader. *Tensor Decompositions and Applications.* SIAM Rev. 51(3) (2009) 455–500.

[27] S. A. Losilla, D. Sundholm, J. Juselius *The direct approach to gravitation and electrostatics method for periodic systems.* J. Chem. Phys. 132 (2) (2010) 024102.

[28] T. Blesgen, V. Gavini, V. Khoromskaia. *Approximation of the electron density of Aluminium clusters in tensor-product format.* J. Comp. Phys. 231(6) (2012) 2551–2564.

[29] G. I. Marchuk and V. V. Shaidurov. *Difference methods and their extrapolations.* Applications of Mathematics, New York: Springer, 1983.

[30] S. Brenner and R. Scott. *The mathematical theory of finite element methods.* Springer, 1994.

[31] L. Genovese, B. Videau, M.Ospici, T. Deutsch, S, Goedecker and J.-F. Méhaut. *Daubechies wavelets for high performance electronic structure calculations: The BigDFT project.* High Perf. Comp., 339(2-3) (2011) 149–164.

[32] S. Östlund and S. Rommer. *Thermodynamics limit of density matrix renormalization.* Phys. Rev. Lett., 75 (1995) 3537–3540.

[33] G. Vidal. *Efficient classical simulation of slightly entangled quantum computations.* Phys. Rev. Lett. 91(14) (2003) 147902-1 147902-4.

[34] I.V. Oseledets, and E.E. Tyrtyshnikov, *Breaking the Curse of Dimensionality, or How to Use SVD in Many Dimensions.* SIAM J. Sci. Comp., 31 (2009), 3744-3759.

[35] S. Holtz, Th. Rohwedder, and R. Schneider. *The manifolds of tensors of fixed TT-rank.* Numer. Math. 120(4), 2012.

[36] B.N. Khoromskij, and I. Oseledets. *Quantics-TT approximation of elliptic solution operators in higher dimensions.* Russ. J. Numer. Anal. Math. Modelling, 26(3) (2011) 303-322.

Molecule, number of basis functions	Element symbol	Nuclear charge number	Coordinates of nuclei		
			X	Y	Z
C_2H_5OH,	C	6	0.0	−1.073130810	−0.034788912
123	C	6	0.0	0.460542651	2.379525493
	O	8	0.0	0.608614000	−2.085184857
	H	1	0.0	−0.317955927	−3.611373598
	H	1	1.669357848	−2.299425057	−0.091952187
	H	1	−1.669357848	−2.299425057	−0.091952187
	H	1	1.670642597	1.667565381	2.461670355
	H	1	−1.670642597	1.667565381	2.461670355
	H	1	0.0	−0.779241493	4.030057328
N_2H_4,	N	7	0.0	1.367699039	0.0
82	N	7	0.0	−1.367699039	0.0
	H	1	1.841335527	1.859207422	0.0
	H	1	−1.841335527	−1.859207422	0.0
	H	1	−0.572853975	1.859207422	1.749958527
	H	1	0.572853975	−1.859207422	−1.749958527
H_2O_2,	O	8	1.315741179	0.0	0.0
68	O	8	−1.315741179	0.0	0.0
	H	1	1.699070297	1.476608885	0.939962179
	H	1	−1.699070297	−1.476608885	0.939962179
CH_4,	C	6	0.0	0.0	0.0
55	H	1	1.18600000	1.18600000	1.18600000
	H	1	−1.18600000	−1.18600000	1.18600000
	H	1	−1.18600000	1.18600000	−1.18600000
	H	1	1.18600000	−1.18600000	−1.18600000
NH_3,	N	7	0.0	0.0	0.0
48	H	1	1.755448702	0.0	−0.738303718
	H	1	−0.877724351	1.520263171	−0.738303718
	H	1	−0.877724351	−1.520263171	−0.738303718
H_2O,	O	8	0.0	0.0	0.0
41	H	1	0.0	0.0	1.809413
	H	1	0.0	1.751699	−0.453346
HF,	F	9	0.0	0.0	0.0
34	H	1	0.0	0.0	1.703600

Table 9.1: Cartesian coordinates of nuclei (in a.u.) used in the molecular electronic structure calculations.